

Artificial DNA-Bending Six-Zinc Finger Peptides with Different Charged Linkers: Distinct Kinetic Properties of DNA Bindings[†]

Miki Imanishi and Yukio Sugiura*

Institute for Chemical Research, Kyoto University, Uji, Kyoto 611-0011, Japan

Received September 5, 2001; Revised Manuscript Received November 13, 2001

ABSTRACT: Many transcription factors are known to induce DNA bending and support the formation of specific DNA architectures. The protein-induced DNA bending is helpful for many combinations of protein–protein and/or –DNA interactions that are necessary for various biological reactions. The kinetic stability of a bent DNA–protein complex has a significant influence on transcriptional efficiency, and hence, such regulation of the kinetic stability is a new concept for transcriptional regulation. We created six-zinc finger proteins [Sp1ZF6(Gly)10, Sp1ZF6(Gr)4, and Sp1ZF6(GE)4] by connecting two DNA binding domains of transcription factor Sp1 with different charged linkers consisting of 10 amino acid residues. Gel mobility shift assays and methylation interference assays revealed that these artificial proteins recognized the expected DNA sequence and that the DNA binding specificities of these three proteins were similar regardless of the difference in the charges or flexibility of the linkers. The phasing analyses suggested that these three zinc finger proteins induced DNA bending in an analogous manner. On the basis of the surface plasmon resonance experiments, however, specific differences in the kinetic properties of DNA binding among these proteins were demonstrated. Of special interest is the fact that the dissociation rate of Sp1ZF6(Gly)10 was faster than that of Sp1ZF6(Gr)4 despite the similarities in the DNA binding mode, the induced DNA structural change, and the association rate. Such DNA-bending six-zinc finger proteins with different stabilities for the bent DNA–protein complexes may be useful as new tools for the kinetic regulation of sequence specific transcription.

In the transcriptional initiation complex, not only specific protein binding but also the DNA architecture is very important. It is known that a protein-induced DNA structural change is indispensable for some interactions between proteins located on distal sites. Therefore, an artificial protein that induces a DNA conformational alteration is interesting as a transcriptional regulator of a specific gene. The recent determination of the three-dimensional structures for several protein–DNA complexes has revealed that the intercalating side chain can distort the DNA (reviewed in ref 1). This bending type was induced by the high-mobility group (HMG) box proteins and the TATA box binding protein (TBP). DNA modification by charge neutralization on the phosphodiester backbone also brought about DNA bending (2–4). Electrostatic effects of the DNA binding of proteins such as bZIP (5–8), *Escherichia coli* CAP (9), or the *Saccharomyces cerevisiae* MATa1 and MATα1 homeodomain proteins (10) play a significant role in the DNA bending. In addition to the importance of the DNA architecture, the relation between the DNA binding kinetics of the DNA-bending proteins and the transcriptional efficiency was recently reported (11). They tested the hypothesis that the kinetic stability of a bent HMG

box–DNA complex can in itself modulate transcriptional potency. Indeed, the kinetic stability resulting from the slower dissociation constant of the bent protein–DNA complex could contribute to the enhancement of the transcription. However, little is known about the kinetics of the DNA-bending proteins. A study on the bendability of the minor helix groove was reported using an artificial DNA-bending agent, a tethered triple-helix-forming oligonucleotide (a tethered TFO), and the bound lifetime of the bent complex was demonstrated to be 2–3-fold shorter than that of the unbent complex (12). In general, DNA binding proteins are able to bind to DNA in a more adaptable manner than the triple-helix-forming oligonucleotides. In various biological reactions, many protein–protein and/or –DNA interactions with different kinetics are mediated by specific DNA architectures. Therefore, it would be helpful for the understanding of such interactions to understand the DNA binding kinetics and the DNA structural change. The design of artificial proteins that induce DNA bending in a kinetically different DNA binding manner is hopefully anticipated for the novel concept of gene regulation.

A zinc finger motif of the C2H2 type, one of the most common DNA binding motifs in eukaryotes, presents an attractive framework for the design of novel DNA binding proteins (13, 14) because of its characteristic DNA binding manner (15). Many artificial zinc finger proteins have been designed for the purpose of the sequence specific regulation of target genes (16–23). To induce a DNA structural change, on the other hand, we have already created artificial six-

[†] This study was supported in part by a Grant-in-Aid for COE Project “Element Science” (12CE2005) and a Grant-in-Aid for Scientific Research (12470505·12793008) from the Ministry of Education, Culture, Sports, Science, and Technology, Japan. M.I. is a research fellow of the Japan Society for the Promotion of Science.

* To whom correspondence should be addressed. Phone: +81-774-38-3210. Fax: +81-774-32-3038. E-mail: sugiura@scl.kyoto-u.ac.jp.

zinc finger proteins, Sp1ZF6(Gly)4, Sp1ZF6(Gly)7, and Sp1ZF6(Gly)10, with 4, 7, and 10 glycine residues as the linkers, respectively (24), by connecting a couple of three-finger DNA binding domains of transcription factor Sp1. Sp1ZF6(Gly)7 and Sp1ZF6(Gly)10 bound to two distal GC boxes with one intervening helical turn and induced DNA bending at the intervening region, though the linker region did not directly contact the DNA bases. It was indicated that the linker length has crucial effects on the DNA bending direction. In this study, we changed the property of the linker of 10 amino acid residues. Namely, the flexible and neutral linker of Sp1ZF6(Gly)10 was converted to charged linkers, including arginine residues or glutamate residues. The effects of the charged linkers on the DNA structure and DNA binding kinetics were examined.

MATERIALS AND METHODS

Chemicals. T4 polynucleotide kinase and restriction enzymes were purchased from New England Biolabs (Beverly, MA). Labeled compound [γ - 32 P]ATP was supplied from DuPont, and dimethyl sulfate was obtained from Aldrich (Milwaukee, WI). The plasmid pBS-Sp1-fl was kindly provided by R. Tjian. All other chemicals were of commercial reagent grade.

Construction of Genes and Peptide Expression. Sp1ZF6(GE)4 and Sp1ZF6(GR)4 were constructed as previously described (24), by exchanging the TGEKP linker region of Sp1ZF6 (23) with the QG(GE)4Q and QG(GR)4Q linkers. These zinc finger peptides were overexpressed in *E. coli* BL21(DE3)pLysS and purified as previously described (23).

Gel Mobility Shift Assays. The 48 bp oligonucleotide containing two distal GC box sequences with 10 bp intervening and the complement oligonucleotide were purchased from Amersham Pharmacia Biotech. The 32 P-labeled oligonucleotide was annealed with the complement oligonucleotide. Gel mobility shift assays were carried out under the following conditions. Each reaction mixture contained 10 mM Tris buffer (pH 8.0), 50 mM NaCl, 5 mM MgCl₂, 1 mM β -mercaptoethanol, 0.05% Nonidet P-40, 5% glycerol, 25 ng/ μ L poly(dI-dC) (Amersham Pharmacia Biotech), the 5'-end-labeled DNA fragment (<50 pM), and 0–300 nM zinc finger proteins. After incubation at 4 °C for 1 h, the sample solutions were electrophoresed on an 8% nondenaturing polyacrylamide gel with Tris-borate buffer [88 mM Tris-HCl (pH 8.0) and 88 mM boric acid] at 4 °C. The bands were visualized using a STORM instrument (Amersham Pharmacia Biotech) and analyzed with ImageQuant software (Molecular Dynamics). The equilibrium dissociation constants (K_d) of each protein–DNA fragment complex were evaluated by fitting the experimentally obtained values of θ_b (the fraction of labeled DNA bound to the protein) to the binding isotherm equation (eq 1) using the KaleidaGraph program (Abelbeck Software).

$$\theta_b = [\text{protein}]/([\text{protein}] + K_d) \quad (1)$$

Methylation Interference Analysis. Methylation interference assays were investigated as described previously (25). The binding reaction was performed under the same conditions as the gel mobility shift assay. To examine both the strong and weak base contacts in the methylation interference experiment, we selected the experimental condition in which

the peptide:DNA molar ratio in the binding reaction is $\sim 10\%$ bound.

Phasing Analysis. Phasing analyses were carried out under the following conditions. Each reaction mixture contained 10 mM Tris buffer (pH 8.0), 50 mM NaCl, 1 mM β -mercaptoethanol, 0.05% Nonidet P-40, 5% glycerol, 34 nM substrate DNA, and 50 nM zinc finger protein. As the substrate DNA, a set of DNA fragments derived from pPhase-GCmixGC-[n] and GCatGC-[n] ($n = 8, 10, 12, 14, 16$, or 18) were used (24). The binding reactions were carried out at 4 °C for more than 1 h, and then the samples were loaded on an 8% polyacrylamide gel (a 74:1 acrylamide:bisacrylamide ratio) with Tris-borate buffer in the absence or presence of 2 mM MgCl₂ at 4 °C. The electrophoretic mobility of each band was normalized to the apparent base pairs (26), and the relative mobilities (R_L) were fitted to the cosine function as previously described (24).

Kinetic Analysis Using Surface Plasmon Resonance. The principle of operation of the BIACORE biosensor has already been described (27). The protein–DNA interaction was studied using a BIACORE X instrument (BIACORE AB, Uppsala, Sweden) operated at 30 °C. The 5'-biotinylated oligonucleotide (5'-biotin-GATATCGGGGCGGGGCTAC-GAGTCCAGGGGCGGGGCATGA-3') was annealed with the complementary strand in flow buffer. The duplex DNA solution was injected over a streptavidin-coated sensor chip (SA5, BIACORE AB) until a suitable level (200–300 RU) was achieved. Flow cell number 1 was left unmodified as the control. Tris-HCl buffer [10 mM Tris-HCl (pH 7.7), 250 mM NaCl, 20 mM MgCl₂, 0.1 mM ZnCl₂, and 0.005% Tween 20] was used as both the flow buffer and the sample preparation buffer. The concentration of a protein was changed from 5 to 800 nM. The association was followed for 5 min and the dissociation for 10 min at a flow rate of 20 μ L/min. The bound protein was eluted from the DNA by several repeats of a short pulse (5 μ L) of the regeneration solution (20 mM EDTA in 50 mM NaOH). Analysis of the data was performed using the evaluation software supplied with the instrument (BIAevaluation version 3.0). R_{\max} was calculated by fitting the equilibrium response (R_{eq}) versus [protein] curve to a 1:1 binding model. The responses of different protein concentrations were normalized using R_{\max} . The dissociation constant (K_d) was calculated by fitting the fraction of the response to eq 2.

$$R_{\text{eq}} = (R_{\max}C)/(C + K_d) \quad (2)$$

where R_{eq} , R_{\max} , and C are the response at equilibrium, the maximum response level, and the protein concentration, respectively. For obtaining the dissociation rate constants (k_{diss}), the following equation (eq 3) was used.

$$R = R_0 \exp[-k_{\text{diss}}(t - t_0)] \quad (3)$$

where R and R_0 are the responses at time t and t_0 , respectively. The association rate constants (k_{ass}) were calculated from k_{diss}/K_d .

RESULTS

Design of Six-Zinc Finger Proteins with Charged Linkers. Novel six-zinc finger proteins, Sp1ZF6(GR)4 and Sp1ZF6(GE)4, were created by linking two three-zinc fingers of transcription factor Sp1 with the GGRGRGRGRQ and GGEGEGEGEQ sequences, respectively (Figure 1). They

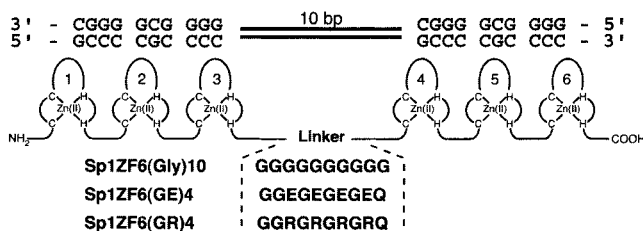


FIGURE 1: Schematic representation of Sp1ZF6(Gly)10, Sp1ZF6(GE)4, and Sp1ZF6(GR)4.

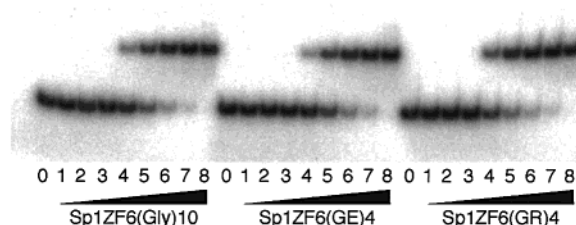


FIGURE 2: Gel mobility shift assays for the Sp1ZF6(Gly)10, Sp1ZF6(GE)4, and Sp1ZF6(GR)4 bindings to the GCmixGC sequence (0, 0.1, 0.3, 1, 3, 10, 30, 100, and 500 nM proteins in lanes 0–8, respectively).

have the same number of linker residues as Sp1ZF6(Gly)10 (24). Therefore, we compared their DNA binding modes with that of Sp1ZF6(Gly)10 from the viewpoints of electrostatic effects and the flexibility of the linker. The DNA binding domain of transcription factor Sp1 strongly binds to the GC (5'-GGGGCGGGC-3') sequence called the GC box (28). The DNA sequence containing two GC boxes with one helical turn intervening was used as the target of the artificial proteins, because Sp1ZF6(Gly)10 has a linker length sufficient to bind to the sequence (24).

DNA Binding Specificity of Artificial Six-Zinc Finger Proteins. To demonstrate whether the artificial six-zinc finger proteins could specifically bind to two distal GC boxes with one intervening helical turn, we performed gel mobility shift assays using a 48 bp duplex fragment containing two distal GC boxes with a 10 bp intervening sequence. As shown in Figure 2, each artificial protein exhibited a single shifted band dependent on the concentration and no other shifted bands were detected, suggesting that each protein formed a single 1:1 complex with the DNA fragment containing two distal GC boxes. The equilibrium dissociation constants (K_d) were calculated on the basis of eq 1. The estimated K_d values of Sp1ZF6(Gly)10, Sp1ZF6(GE)4, and Sp1ZF6(GR)4 were 9.2, 14.3, and 5.6 nM, respectively. Although the differences in the equilibrium dissociation constant of each protein were not significant, the affinity of Sp1ZF6(GR)4 was reproducibly the highest and that of Sp1ZF6(GE)4 was also the lowest. The specificity of their base recognition was examined by methylation interference analyses. This method detects specific guanine bases that play an important role in the formation of the protein–DNA complex. Sp1ZF6(Gly)-10, Sp1ZF6(GE)4, and Sp1ZF6(GR)4 presented the contacts with guanine bases in both of the two GC boxes, and the DNA recognition specificity of each protein seemed to be very similar (Figure 3). On the basis of the results from the gel mobility shift assays and the methylation interference assays, it was suggested that Sp1ZF6(Gly)10, Sp1ZF6(GE)4, and Sp1ZF6(GR)4 bound to both GC boxes in a similar manner, but their K_d values were slightly different.

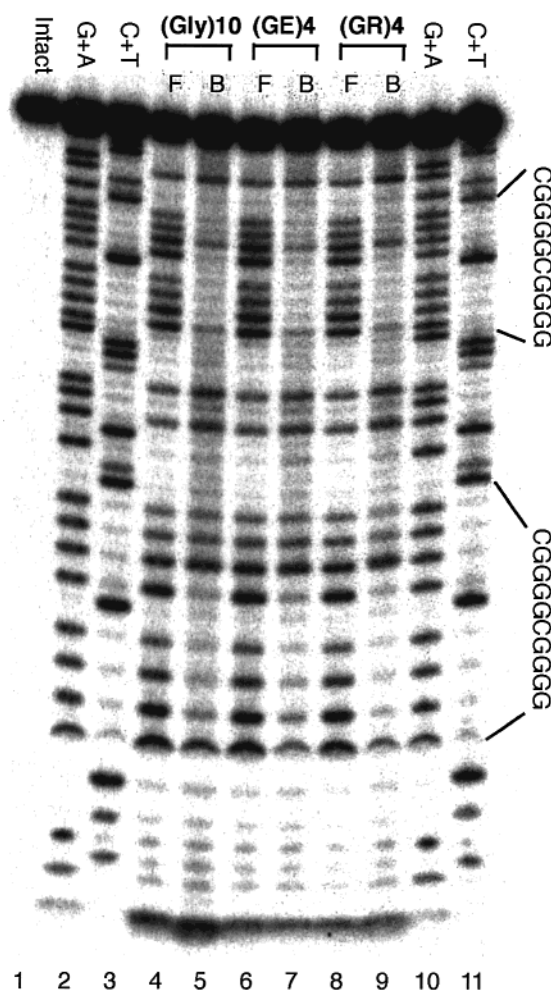


FIGURE 3: Methylation interference analyses for Sp1ZF6(Gly)10, Sp1ZF6(GE)4, and Sp1ZF6(GR)4 bindings to the GCmixGC sequence. Lanes 4–9 show free (F) and protein-bound (B) DNA samples. Lanes 2 and 10 show G+A of the Maxam–Gilbert sequencing reaction and lanes 3 and 11 C+T, and lane 1 shows intact DNA.

DNA Structural Change Induced by Binding of Artificial Six-Zinc Finger Proteins. To test the effects of the charge and flexibility of the linker on the DNA structural change, we performed phasing analyses. This method is utilized for the highly sensitive detection of DNA bending. It is based on the phase-dependent interaction between a protein-induced DNA bend and a reference DNA bend localized on the same DNA fragment (29). A set of phase-sensitive DNA fragments termed GCmixGC or GCatGC were used to examine the effect of the sequence-dependent DNA bending (24). Both sequences have two distal GC boxes with 10 intervening base pairs. However, the intervening sequences, namely, a random sequence (mix) or AT rich sequence (at), were different from each other. As described previously (24), the phase-sensitive DNA fragment contained the protein binding sequence, an array of six phased A_6 tracts with 108° of bending toward the DNA major groove in the center (30), and a varied spacer length between them from 8 to 18 bp in increments of 2 bp. If DNA bending were to occur at the protein binding site, the overall shape of the DNA fragment would be altered by the spacer length in the range of conformational isomers between the in-phase and the out-of-phase orientations of the reference and the induced bend (31). The DNA structural change can be estimated from the difference in mobility for

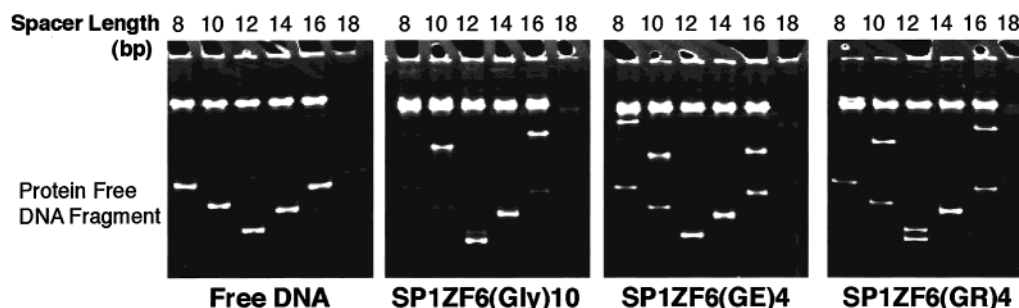


FIGURE 4: Results of the phasing analyses for the Sp1ZF6(Gly)10, Sp1ZF6(GE)4, and Sp1ZF6(GR)4 bindings to the phasing DNA fragments with the GCmixGC sequence. Both protein-free and protein-bound bands were detected.

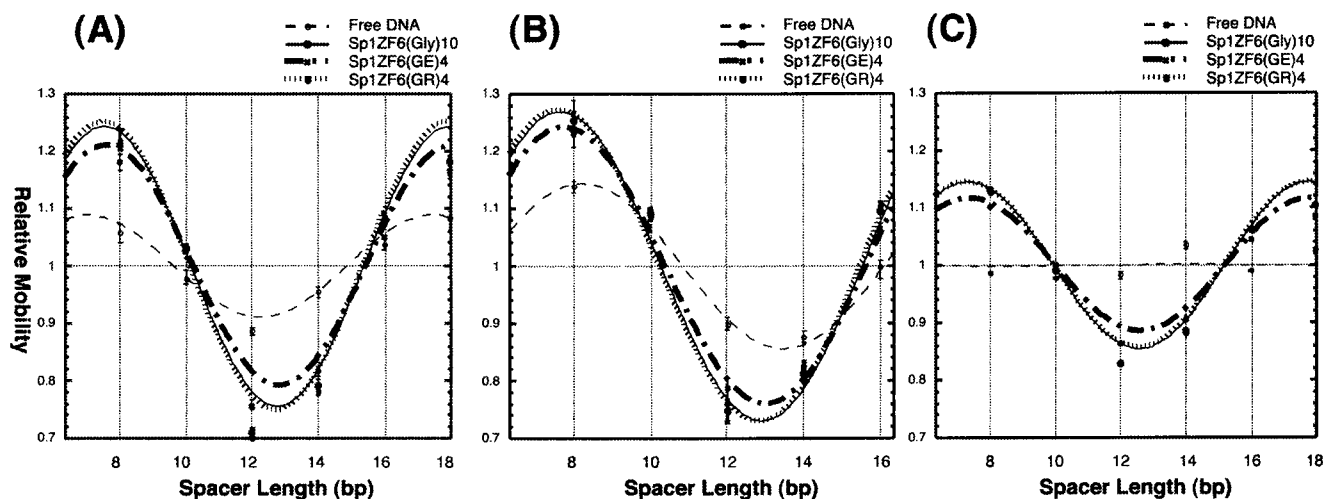


FIGURE 5: Cosine curves of the plot of relative mobility vs spacer length. The protein binding sequences were GCmixGC (A and C) and GCatGC (B). The cosine curves are based on the results of the phasing analyses for each protein electrophoresed in the absence (A and B) or presence (C) of 2 mM MgCl_2 . The electrophoretic mobility of the phasing DNA fragments is plotted vs spacer length. Data were normalized to the average mobility over the entire spacer range.

a set of phase-dependent fragments. Figure 4 summarizes the results of the phasing analysis using the GCmixGC sequence as the target. The relative electrophoretic mobility of a set of phase-sensitive DNA fragments was expressed as the cosine function of the spacer length (32). The data were analyzed by converting each mobility into the corresponding relative mobility and by fitting a cosine function (Figure 5). The amplitude and the phasing obtained from the fitted cosine curves reflect the overall bending magnitude and the bending direction of the protein binding site, respectively. The cosine curve of the GCmixGC complex with Sp1ZF6(GR)4 was almost the same as that with Sp1ZF6(Gly)10, and that with Sp1ZF6(GE)4 exhibited almost the same amplitude but with a slight difference (Figure 5A). An analogous tendency was also obtained when each protein bound to GCatGC sequences (Figure 5B). Interestingly, in both cases of the DNA substrates, GCmixGC and GCatGC, the cosine curves of each protein were very similar regardless of the intervening sequences, although the cosine curves of the protein-free DNA fragments were evidently different from each other. It is known that the DNA flexibility is influenced by the existence of cations (33). To confirm the effects of Mg^{2+} on the DNA structure, we carried out the phasing analysis under the same conditions except using a running buffer containing 2 mM MgCl_2 . Although the sequence-dependent intrinsic DNA bending was rather released, interestingly, all six-zinc finger proteins similarly induced DNA bending with each other even under the different condition (Figure 5C).

Kinetic Analysis Using Surface Plasmon Resonance. To examine whether the charge of the linker region has any influence on the DNA binding, the kinetic aspects of the binding reaction were analyzed using a BIACORE X instrument with GCmixGC DNA immobilized on the surface. This method can monitor the protein–DNA interactions in real time, in contrast to the gel mobility shift assay that detects the protein–DNA interactions under the equilibrium condition. A typical sensorgram is shown in Figure 6A. The measured equilibrium dissociation constants (K_d) were determined by fitting the normalized equilibrium responses of several concentrations of proteins to eq 2 (Figure 6B). The K_d values of 7.03×10^{-8} M for Sp1ZF6(Gly)10 and 8.75×10^{-8} M for Sp1ZF6(GE)4 were similar. On the other hand, the K_d value of 1.18×10^{-8} M for Sp1ZF6(GR)4 was ~ 7 times smaller than that of Sp1ZF6(GE)4. To evaluate the nature of their K_d values, we calculated the dissociation rate constant (k_{diss}) and the association rate constant (k_{ass}) from the sensorgrams. The k_{diss} values were directly estimated from the dissociation rate of the sensorgrams based on eq 3 and the k_{ass} values from k_{diss}/K_d (Table 1). Unexpectedly, the binding kinetics of Sp1ZF6(GR)4 showed no clear characteristics for both the on-rate and off-rate; that is, the k_{ass} value of $2.02 \times 10^4 \text{ M}^{-1} \text{ s}^{-1}$ for Sp1ZF6(GR)4 was similar to the value of $1.17 \times 10^4 \text{ M}^{-1} \text{ s}^{-1}$ for Sp1ZF6(Gly)10, and the k_{diss} value of $2.40 \times 10^{-4} \text{ s}^{-1}$ for Sp1ZF6(GR)4 was close to the value of $4.21 \times 10^{-4} \text{ s}^{-1}$ for Sp1ZF6(GE)4. As for the association phase, Sp1ZF6(GE)4 evidently exhibited a smaller k_{ass} value than the other two proteins, and as for the

Table 1: Association and Dissociation Rate Constants of Sp1ZF6(Gly)10, Sp1ZF6(GE)4, and Sp1ZF6(GR)4 with GCmixGC and GC Sequences

DNA	protein	k_{diss} (s^{-1})	k_{ass} ($\text{M}^{-1} \text{s}^{-1}$)	K_d (M)
GCMixGC	Sp1ZF6(Gly)10	$(8.24 \pm 0.33) \times 10^{-4}$	$(1.17 \pm 0.05) \times 10^4$	$(7.03 \pm 0.06) \times 10^{-8}$
	Sp1ZF6(GE)4	$(4.21 \pm 0.99) \times 10^{-4}$	$(4.79 \pm 0.65) \times 10^3$	$(8.75 \pm 1.46) \times 10^{-8}$
	Sp1ZF6(GR)4	$(2.40 \pm 0.39) \times 10^{-4}$	$(2.02 \pm 0.25) \times 10^4$	$(1.18 \pm 0.13) \times 10^{-8}$
GC	Sp1ZF6(Gly)10	$(9.01 \pm 0.55) \times 10^{-4}$	$(1.05 \pm 0.51) \times 10^4$	$(8.74 \pm 1.00) \times 10^{-8}$
	Sp1ZF6(GE)4	$(3.64 \pm 0.49) \times 10^{-4}$	$(4.38 \pm 0.06) \times 10^3$	$(8.26 \pm 0.27) \times 10^{-8}$
	Sp1ZF6(GR)4	$(3.21 \pm 0.20) \times 10^{-4}$	$(1.52 \pm 0.14) \times 10^4$	$(2.11 \pm 0.23) \times 10^{-8}$

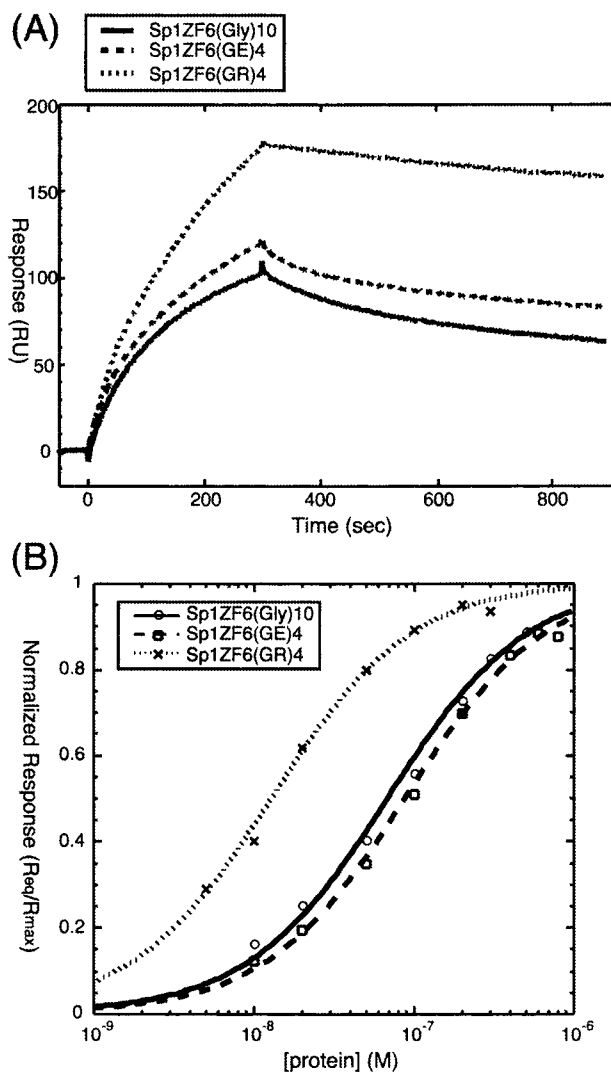


FIGURE 6: (A) Sensorgrams for the binding of 50 nM Sp1ZF6(Gly)10, 50 nM Sp1ZF6(GE)4, and 20 nM Sp1ZF6(GR)4 to the GCmixGC sequence. (B) Determination of the measured equilibrium dissociation constants (K_d) by fitting data for a 1:1 binding model. The equilibrium responses of several concentrations of proteins were normalized using the fitted value for the maximum response.

dissociation phase, Sp1ZF6(Gly)10 had a significantly larger k_{diss} value. These tendencies were also detected using an immobilized DNA containing only one GC box sequence (Table 1).

DISCUSSION

The result of the gel mobility shift assays revealed the DNA binding mode of each zinc finger protein. These six-zinc finger proteins contain two GC box-binding units. Therefore, they can bind to two distal GC boxes at least

three binding modes: (1) one protein binding to two sites, (2) one protein binding to only one site at the low protein concentration, and (3) two protein molecules binding to two sites at the high protein concentration. The observed single shifted band suggests that each protein formed a single 1:1 complex with the DNA fragment containing two distal GC boxes. The values of the equilibrium dissociation constants (K_d) for each protein to the GCmixGC sequence were similar, while the affinity of Sp1ZF6(GR)4 was slightly higher than those of Sp1ZF6(Gly)10 and Sp1ZF6(GE)4. The result of the methylation interference assays showed that the artificial six-zinc finger proteins recognize the guanine bases in the two GC boxes, as shown in the binding of the three-finger wtSp1(530–623) to a GC box sequence (34). The similar recognition manners of these six-finger proteins indicate that the linker region has little effect on the recognition mode.

The phasing analysis detects the DNA structural change induced by the binding of each protein. DNA modification by asymmetrical charge neutralization at the phosphodiester backbone has been demonstrated to bring about DNA bending (2–4). If the linker region interacts with one side of the phosphodiester backbone, the binding of a protein would induce DNA bending. All artificial proteins induced DNA structural changes. The DNA bending patterns induced by Sp1ZF6(GR)4 and by Sp1ZF6(Gly)10 were almost identical, and that induced by Sp1ZF6(GE)4 exhibited an extremely similar but a slightly smaller amplitude. An analogous tendency was also obtained for each protein bound to the GCatGC sequences. In both substrate DNA sequences, the cosine curves of each protein were very similar regardless of the intervening sequences, although those of the protein-free DNA fragments were evidently different from each other. Presumably, the linker charges had little effect on the interaction with the DNA backbone, or they randomly interact with the DNA under the equilibrium condition. The length rather than the property of the linker appears to influence the DNA structure, and the protein-binding structure of two distal GC boxes seems to be independent of the intervening DNA sequence.

When using the running buffer with MgCl_2 , Sp1ZF6(GR)4 and Sp1ZF6(Gly)10 induced almost the same DNA structural change, and Sp1ZF6(GE)4 also had a conformational alteration similar to those of Sp1ZF6(GR)4 and Sp1ZF6(Gly)10, though the magnitude of the amplitude of their cosine curves was smaller than that in the case without MgCl_2 . On the other hand, the sequence-dependent DNA bending was released by the existence of the Mg^{2+} ion, suggesting that the protein-free DNA structure itself is appreciably stabilized. The interactions between each six-finger protein and the DNA fragment were not influenced by the existence of the Mg^{2+} ion, and also, the decrease in the amplitude probably resulted from the DNA stabilization. Strauss et al. (2) pointed

out that the DNA bending induced by asymmetric phosphate neutralization is reversed by the addition of multivalent cations such as Mg^{2+} , Co^{3+} , and spermine. This result supports the fact that the electrostatic effect between the linkers of the six-finger proteins and the DNA phosphate backbone plays an unimportant role in the protein-induced DNA bending.

The kinetic aspects of the binding reaction were analyzed using surface plasmon resonance. Two characteristic features of the association and dissociation processes were clarified. The association rate constant of Sp1ZF6(GE)4 was smaller than those of Sp1ZF6(GR)4 and Sp1ZF6(Gly)10, suggesting the repulsive effect of the negatively charged linker on the association step. It is also possible that the folding of Sp1ZF6(GE)4 is changed because of the interaction between the glutamates and divalent cations. On the other hand, Sp1ZF6(Gly)10 exhibited the fastest dissociation rate concerning the off-rate. It is indicated that the entropic factors due to the flexibility of the linker rather than the charge repulsive effect strongly influence the dissociation from DNA. In contrast with the close equilibrium dissociation constants of the DNA binding of these proteins measured from the gel mobility shift assay, the dissociation constant (K_d) of Sp1ZF6(GR)4 detected by the kinetic analysis was significantly smaller than those of the other two six-finger proteins. Because the time scale of the BIACORE experiments is much shorter than that of the gel mobility shift assays, the binding reaction monitored by the BIACORE studies unlikely represents the formation of a specific complex. The possibility is also supported by the fact that the kinetic aspects of complex formation of each six-finger protein with the GC and GCmixGC sequences are essentially identical, as observed for Sp1ZF9 (23). Nonspecific interactions between the negatively charged DNA and the linker region of Sp1ZF6(GR)4 probably contribute to the slight increase in the association rate and to the decrease in the dissociation rate, resulting in the smallest K_d value. On the basis of the result of the phasing analysis, it is suggested that neither the negatively nor positively charged linker directly interacts with the DNA under the equilibrium condition. Therefore, both charged linkers of Sp1ZF6(GE)4 and Sp1ZF6(GR)4 seem to nonspecifically interact with DNA during the nonequilibrium phase of the binding reaction. This may be responsible for the slight differences in affinities of each protein–GCmixGC DNA complex obtained from the gel mobility shift assays.

It is of special interest that the dissociation rate of Sp1ZF6(Gly)10 was more than 3 times faster than that of Sp1ZF6(GR)4 despite the similarities in the DNA binding mode, the induced DNA structural change, and the association rate constant. The stability of the drug–DNA complex has been shown to affect the transcriptional efficiency (35, 36). The slowly dissociating drugs resulted in complete termination of transcription by the phage RNA polymerase at every occupied site. Very recently, Ukiyama et al. (11) also suggested that the kinetic stability of a bent SRY protein–DNA complex can regulate its transcriptional potency. SRY is a member of the family of HMG box proteins that induce DNA bending that is indispensable for the formation of the transcriptional initiation complex. The chimpanzee SRY that was used has one amino acid substitution compared to human SRY. In comparison with the human SRY, the chimpanzee

SRY shows identical equilibrium properties, such as DNA binding specificity and induced DNA bending, except for the prolonged lifetime with DNA. The 3–4-fold prolonged lifetime of the chimpanzee SRY–DNA complex resulted in an enhancement of the transcription. These results suggest that the kinetic lifetime of the bent SRY–DNA complex regulates the overall lifetime of the enhanceosome. Therefore, it is of interest to kinetically regulate gene expression by the artificial DNA-bending six-zinc finger proteins with different linkers and different dissociation rate constants.

In conclusion, the artificial six-zinc finger proteins presented here, Sp1ZF6(Gly)10, Sp1ZF6(GR)4, and Sp1ZF6(GE)4, induced DNA bending. The DNA recognition mode and the induced DNA structural change were similar among these three six-finger proteins. However, the kinetic aspects of their DNA bindings were clearly different from each other. In particular, the dissociation rate of Sp1ZF6(Gly)10 was the fastest and that of Sp1ZF6(GR)4 was the slowest. The kinetic stability of a bent DNA–protein complex is very important for the assembly of many molecules in various biological reactions. These DNA-bending six-zinc finger proteins may be useful as new tools for the kinetic regulation of the sequence specific transcription.

REFERENCES

1. Werner, M. H., Gronenborn, A. M., and Clore, G. M. (1996) *Science* 271, 778–784.
2. Strauss, J. K., and Maher, L. J., III (1994) *Science* 266, 1829–1834.
3. Strauss, J. K., Vaghefi, M. M., Hogrefe, R. I., and Maher, L. J., III (1997) *Biochemistry* 36, 8692–8698.
4. Strauss, J. K., Roberts, C., Nelson, M. G., Switzer, C., and Maher, L. J., III (1996) *Proc. Natl. Acad. Sci. U.S.A.* 93, 9515–9520.
5. Leonard, D. A., Rajaram, N., and Kerppola, T. K. (1997) *Proc. Natl. Acad. Sci. U.S.A.* 97, 4913–4918.
6. Strauss, J. K., and Maher, L. J., III (1997) *Biochemistry* 36, 10026–10032.
7. Paolella, D. N., Liu, Y., Fabian, M. A., and Schepartz, A. (1997) *Biochemistry* 36, 10033–10038.
8. Strauss, J. K., and Maher, L. J., III (1998) *Biochemistry* 37, 1060–1066.
9. Schultz, S. C., Shields, G. C., and Steitz, T. A. (1991) *Science* 253, 1001–1007.
10. Li, T., Mead, J., Wolberger, C., and Vershon, A. K. (1995) *Science* 270, 262–269.
11. Ukiyama, E., Jancso-Radek, A., Li, B., Milos, L., Zhang, W., Phillips, N. B., Morikawa, N., King, C.-Y., Chan, G., Haqq, C. M., Radek, J. T., Poulat, F., Donahoe, P. K., and Weiss, M. A. (2001) *Mol. Endocrinol.* 15, 363–377.
12. Akiyama, T., and Hogan, M. E. (1996) *J. Biol. Chem.* 271, 29126–29135.
13. Pabo, C. O., Peisach, E., and Grant, R. A. (2001) *Annu. Rev. Biochem.* 70, 313–340.
14. Imanishi, M., Hori, Y., Nagaoka, M., and Sugiura, Y. (2001) *Eur. J. Pharm. Sci.* 13, 91–97.
15. Pavletich, N. P., and Pabo, C. O. (1991) *Science* 252, 809–817.
16. Rebar, E. J., and Pabo, C. O. (1994) *Science* 263, 671–673.
17. Greisman, H. A., and Pabo, C. O. (1997) *Science* 275, 657–661.
18. Jamieson, A. C., Wang, H., and Kim, S.-H. (1996) *Proc. Natl. Acad. Sci. U.S.A.* 93, 12834–12839.
19. Choo, Y., Castellanos, A., García-Hernández, B., Sánchez-García, I., and Klug, A. (1997) *J. Mol. Biol.* 273, 525–532.

20. Kim, J.-S., and Pabo, C. O. (1998) *Proc. Natl. Acad. Sci. U.S.A.* 95, 2812–2817.
21. Liu, Q., Segal, D. J., Ghiara, J. B., and Barbas, C. F., III (1997) *Proc. Natl. Acad. Sci. U.S.A.* 94, 5525–5530.
22. Beerli, R. R., Segal, D. J., Dreier, B., and Barbas, C. F., III (1998) *Proc. Natl. Acad. Sci. U.S.A.* 95, 14628–14633.
23. Kamiuchi, T., Abe, E., Imanishi, M., Kaji, T., Nagaoka, M., and Sugiura, Y. (1998) *Biochemistry* 37, 13827–13834.
24. Imanishi, M., Hori, Y., Nagaoka, M., and Sugiura, Y. (2000) *Biochemistry* 39, 4383–4390.
25. Kuwahara, J., Yonezawa, A., Futamura, M., and Sugiura, Y. (1993) *Biochemistry* 32, 5994–6001.
26. Liberles, D. A., and Dervan, P. B. (1996) *Proc. Natl. Acad. Sci. U.S.A.* 93, 9510–9514.
27. Jönsson, U. D., Fägerstam, L., Ivarsson, B., Lundh, K., Löfas, S., Persson, B., Roos, H., Rönnberg, J., Sjölander, S., Stenberg, E., Stahlberg, R., Urbaniczky, C., Östlin, H., and Malmqvist, M. (1991) *BioTechniques* 11, 620–627.
28. Kadonaga, J. T., Carmer, K. R., Masiarz, F. R., and Tjian, R. (1987) *Cell* 51, 1079–1090.
29. Zinkel, S. S., and Crothers, D. M. (1987) *Nature* 328, 178–181.
30. Crothers, D. M., Haran, T. E., and Nadeau, J. G. (1990) *J. Biol. Chem.* 265, 7093–7096.
31. Akiyama, T., and Hogan, M. E. (1997) *Biochemistry* 36, 2307–2315.
32. Kerppola, T. K., and Curran, T. (1991) *Cell* 66, 317–326.
33. Harrington, R. E. (1978) *Biopolymers* 17, 919–936.
34. Yokono, M., Saegusa, N., Matsushita, K., and Sugiura, Y. (1998) *Biochemistry* 37, 6824–6832.
35. White, R. J., and Phillips, D. R. (1988) *Biochemistry* 27, 9122–9132.
36. White, R. J., and Phillips, D. R. (1989) *Biochemistry* 28, 4277–4283.

BI011761X